Analytical Methods

ROYAL SOCIETY OF CHEMISTRY

PAPER

View Article Online
View Journal

Cite this: DOI: 10.1039/d1ay00782c

Quantification of chromogranin A using a surface plasmon resonance-based biosensor

Yang Xiao,†[ab] Yang Tai, †[ab] Xin Quan,[ab] Chong Zhao,[ab] Rui Liu,[ab] Huan Tong,[ab] Zhiyin Huang,[b] Chengwei Tang[ab] and Jinhang Gao *[ab]

The chromogranin A (CgA) level in the blood is an important biomarker for neuroendocrine tumors and other diseases. Traditional methods for detecting CgA are expensive and time-consuming with low reproducibility. In this study, surface plasmon resonance (SPR), a simple and label-free technique, was validated for quantifying CgA. CgA antibody (CgA-Ab) was immobilized on the CM5 sensor chip (CgA-Ab-CM5) at optimal conditions (pH 5.0, 10 μg mL^{-1}). Next, different concentrations of CgA were measured by CgA-Ab-CM5. The binding and regeneration conditions were optimized and used in each measurement. A binding time of 240 s, and flow rate of 30 μL min^{-1} were chosen as the optimal binding conditions. A pH of 1.75 was the optimal regeneration condition. Compared to the detection range of 23.4–187 ng mL^{-1} for enzyme-linked immunosorbent assay (ELISA), a linear range of 0.2–187 ng mL^{-1} was detected based on the response unit (RU), showing high sensitivity and reliability of SPR. Finally, the reproducibility of the CgA-Ab-CM5 chip was accessed by consecutive binding-regeneration cycles for 300 times. In conclusion, the SPR-based CgA-Ab-CM5 chip is a sensitive and reproducible method for quantifying CgA levels in a real-time manner.

Received 8th May 2021
Accepted 29th July 2021

DOI: 10.1039/d1ay00782c

rsc.li/methods

1 Introduction

Human chromogranin A (CgA), an acidic glycoprotein consisting of 439 residues, belongs to a regulated secretory protein family called granins.[1] It has been primarily discovered from the stimulated adrenal medulla in 1965 and has been demonstrated to be a circulating biomarker for a wild range of human neuroendocrine tumors (NETs) immediately afterwards.[2,3] A high sensitivity (90%) and specificity (92%) of plasma CgA level in the diagnosis of pheochromocytoma/paraganglioma with the cut-off value of 150 ng mL^{-1} have been reported recently.[4] The CgA level returns to normal levels (59.2–76.0 ng mL^{-1}) after surgery in 99% of patients, suggesting that the CgA level may be connected with tumor burden.[4] Another study also found that a high level of CgA (over 94 μg L^{-1}) is associated with a higher rate of metastasis in pancreatic ductal adenocarcinoma and shorter survival.[5] Therefore, the quantification of CgA in the bloodstream is urgently needed for the diagnosis and prognosis evaluation of NETs.

Recently, enzyme-linked immunosorbent assay (ELISA), immunoradiometric assay (IRMA), and radioimmunoassay (RIA) are wildly used in the quantification of CgA in serum/plasma.[6,7] Nevertheless, some limitations make these methods unavailable for routine clinical tests. The common disadvantages are the need for specific label agents as detection targets and time consumption.[8] RIA and IRMA are expensive for high labor requirements and suffer from exposure to hazardous radioisotops.[9] Further, IRMA has been shown lower sensitivity than ELISA in diagnosing NETs with CgA. It is probably because IRMA requires two antibodies recognizing the central part of CgA, while different proteolytic processes may occur during the synthesis of CgA.[10] However, ELISA also involves multiple washing steps and long reaction times without automation and low reproducibility. These limitations of the current methods inspired us to find a straightforward approach for the real-time quantification of CgA.

Surface plasmon resonance (SPR) is an optical technique used to detect molecular interactions.[11] The biosensor coats the antigen and the amount of the analyte positively correlate with the response unit (RU) *via* refractive index.[12] SPR can monitor biological and chemical analytes in a real-time and label-free method with advantages of high sensitivity, selectivity, and reproducibility.[13] SPR-based techniques combined with other techniques, such as immune sensors, imaging, and microscopy are wildly used in basic science, diagnostic assays, and drug development.[12] Our previous studies have applied somatostatin and its receptors combined with a CM5 sensor chip to quantify somatostatin and detect the affinity between somatostatin and its receptors,[14] demonstrating the potential of SPR for clinical

[a]*Lab of Gastroenterology and Hepatology, West China Hospital, Sichuan University, NO. 1, 4th Keyuan Road, Chengdu, 610041, People's Republic of China. E-mail: Gao.jinhang@qq.com; Fax: +86-28-85582944; Tel: +86-28-85164011*

[b]*Department of Gastroenterology, West China Hospital, Sichuan University, Chengdu, China*

† Yang Xiao and Yang Tai contributed equally to this study.

real-time quantifying somatostatin as a simple, sensitive, and reproducible method.[15]

In the current study, we attempted to quantify CgA in a simple, sensitive, and real-time approach using the SPR-based BIAcore technique. BIAcore displayed its simplicity of operation, high sensitivity, and reliability in detecting CgA with a quantification range of 0.2–187 ng mL^{-1}.

2 Materials and methods

2.1 Reagents and equipment

CgA and CgA ELISA kits were purchased from R&D Systems (Minneapolis, MN, USA), and CgA antibody (CgA-Ab) was purchased from Santa Cruz (Dallas, TX, USA). Two-channel CM5 sensor chips coated with carboxymethylated dextran layer, coupling buffer (10 mM sodium acetate, pH 4.0, 4.5, 5.0, 5.5), running and sample buffers (HBS-EP; 0.01 M HEPES, pH 7.4; 0.15 M NaCl; 3 mM EDTA; 0.005% surfactant polysorbate 20), amine-coupling reagents (0.05 M *N*-hydroxysuccinimide [NHS], 0.2 M *N*-ethyl-*N*′-(3-diethylaminopropyl) carbodiimide [EDC]), ethanolamine–HCl (1 M, pH 8.5) and regeneration solutions (1 M glycine–HCl, pH 1.5, 2.0, 2.5, 3.0) were purchased from Biacore AB (Uppsala, Sweden). Data were obtained using a Biacore X biosensor (Biacore AB).

2.2 Optimization of coupling conditions

The CgA-Ab was prepared with different coupling buffers (10 mM sodium acetate, pH 4.0, 4.5, 5.0, and 5.5) and then injected into the flow channel 2 (FC2) of the CM5 sensor chip with the same concentration (5 μg mL^{-1}). The optimum coupling pH was determined based on the maximal RU. Next, various concentrations of CgA-Ab (5, 10, 15, 20, 25 μg mL^{-1}) diluted in sodium acetate with determined optimal pH (5.0) were injected into FC2. The optimal concentration of the coupling receptor was measured according to maximal RU. All experiments above were carried out at a flow rate of 10 μL min^{-1} for 2 minutes and a temperature of 25 °C.

2.3 Immobilization of CgA antibody on the surface of CM5 sensor chips

The CM5 sensor chips need to be activated before immobilization. 0.4 M EDC and 0.1 M NHS were proportionally mixed (1 : 1, v/v). The mixture was injected into FC1 and FC2 sequentially with a flow rate of 5 μL min^{-1} for 7 minutes to activate the carboxymethylated dextran layers. Then, CgA-Ab at the optimal pH and concentration was coupled to FC2 surfaces *via* its free amines at a flow rate of 5 μL min^{-1} for 7 minutes (CgA-Ab-CM5). FC1 was regarded as a reference channel. After coupling, the remaining unreacted sites on both flow channels were blocked by ethanolamine–HCl at a flow rate of 5 μL min^{-1} for 7 min. Finally, glycine–HCl (1 M, pH 2.5) was injected into the flow channel at a rate of 5 μL min^{-1} for 1 min to wash and regenerate immobilized surfaces.

2.4 Optimization of the binding and regenerating conditions

CgA was diluted at the same concentration of 5.9 ng mL^{-1} using HBS-EP buffer. After immobilization, the prepared CgA was injected into both flow channels at the same flow rate, and sensorgrams were recorded at different times (360, 300, 240, 180, 120 s) of interaction between CgA and CgA-Ab-CM5. The optimal binding time was obtained according to RU. Next, by injecting CgA at different flow rates (5, 10, 20, 30, 40 μL min^{-1}) with the same reaction time, the optimal binding flow rate was determined. After interacting with CgA, the surfaces of FC1 and FC2 were regenerated by 1 M glycine–HCl at different pH (3.0, 2.5, 2.0, 1.75, 1.5). Then, the optimal regeneration pH was obtained as well.

2.5 Quantification of CgA

The CgA was diluted in HBS-EP buffer at various concentrations ranging from 0.2–187 ng mL^{-1} at 25 °C. Then, the samples were injected into FC1 and FC2 at a flow rate of 30 μL min^{-1} for 4 minutes. HBS-EP was used as a negative control. Each time after injecting, the surfaces of the flow channel were regenerated with 1 M glycine–HCl (pH 1.75) at a flow rate of 30 μL min^{-1} for 30 seconds.

2.6 Reproducibility and reusable times of CgA-Ab-CM5 chip

The consecutive binding-regeneration cycles were carried out to assess the reusing and reproducibility of the CgA-Ab-CM5 chip. For reproducibility, CgA at different concentrations (5.9, 42, 187 ng mL^{-1}) were injected into FC1 and FC2 at a flow rate of 30 μL min^{-1} for 4 minutes. Then the surfaces were regenerated each time with the regeneration solution (1 M glycine–HCl, pH 1.75) at a flow rate of 30 μL min^{-1} for 30 seconds. The reuse capability of the CgA-Ab-CM5 chip with CgA at 5.9 ng mL^{-1} was tested after 20, 60, 100, 140, 180, 220, 260, and 300 cycles of regeneration. Similarly, the reuse capability of the CgA-Ab-CM5 chip with CgA at 42 ng mL^{-1} and 187 ng mL^{-1} were tested after 1, 40, 80, 120, 160, 200, 240, 280 and 10, 50, 90, 130, 170, 210, 250, 290 cycles of regeneration, respectively.

2.7 Data processing and analysis

The data were analyzed using Evaluation software version 4.1 (Biacore AB). Each sample was repeatedly tried 3 times, and quantitative data were presented as mean ± standard deviation. All the data were double referenced with FC1 and HBS-EP buffer. The FC1 sensorgrams were automatically subtracted from FC2. For data analysis, the signal was initially X zeroed at the beginning of the association phase. Then, all curves were Y transformed, and the negative control responses (HBS-EP buffer) were subtracted from each entire dataset.

2.8 ELISA for CgA

The CgA was diluted in HBS-EP buffer at various concentrations ranging from 0.2–187 ng mL^{-1} at 25 °C. Then, the CgA was quantified with ELISA kits according to the manufacturer's instructions. Briefly, the CgA dilution and standards were

incubated with ELISA plates for 2 hours at 37 °C, and the unbound substances were removed by washing with PBS. Then a detection antibody was added and incubated for 1 hour at 37 °C. After washing with PBS, the HRP substrate was added and incubated for 30 minutes at 37 °C, followed by a stop buffer. Finally, the absorbance of each well was determined immediately using a microplate reader set to 450 nm. The absorbance was used to create calibration curves.

3 Results and discussion

3.1 Optimization of the coupling conditions

The coating antibody was coupled with a CM5 sensor chip and provided binding sites for analytes. When the amount of analytes is more than that of the coated antibody, the RU in the sensorgrams will reach a plateau, and RU will no longer increase with the increasing amount of analytes.[16] Therefore, the amount of CgA-Ab coupled with the CM5 sensor chip directly affects the upper limit of detection, and the coupling condition should be optimized first. After activation by EDC/NHS, covalent binding sites of carboxyl dextran were activated to bind CgA-Ab. During this coupling process, the pH and concentration are key factors affecting immobilization. Different pH values of the coupling buffer (10 mM sodium acetate, pH 4.0, 4.5, 5.0, 5.5) were chosen based on the isoelectric point of a carboxymethyl dextran and CgA-Ab. CgA-Ab coupled with the CM5 sensor chip at a pH of 5.0 produced the highest RU (Fig. 1A and B), suggesting that the optimal immobilization pH of CgA-Ab was 5.0.

As shown in Fig. 1C and D, RU increases significantly as the concentration of CgA-Ab increases from 5–10 μg mL^{-1}. However, there was a minor increase when the concentration was more than 10 μg mL^{-1}, so we determined the optimal

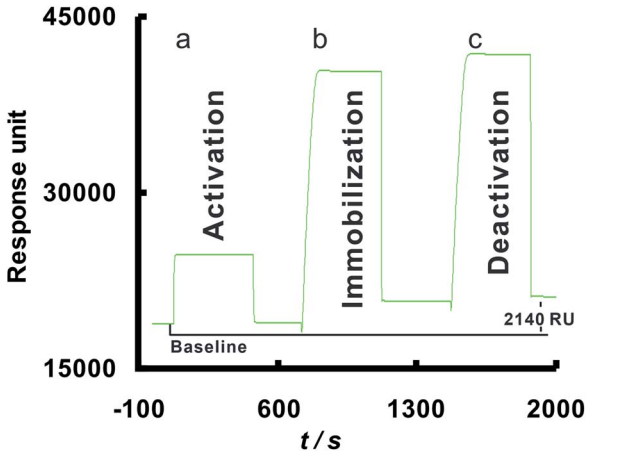

Fig. 2 Amine coupling of CgA-Ab on CM5 sensor chip as shown in the sensorgrams, the CM5 sensor chip has processed an activation (a), immobilization (b), and deactivation (c) cycle. Finally, an immobilization signal of 2140 RU was obtained by subtracting the RU value of baseline from the RU value after the amine coupling process.

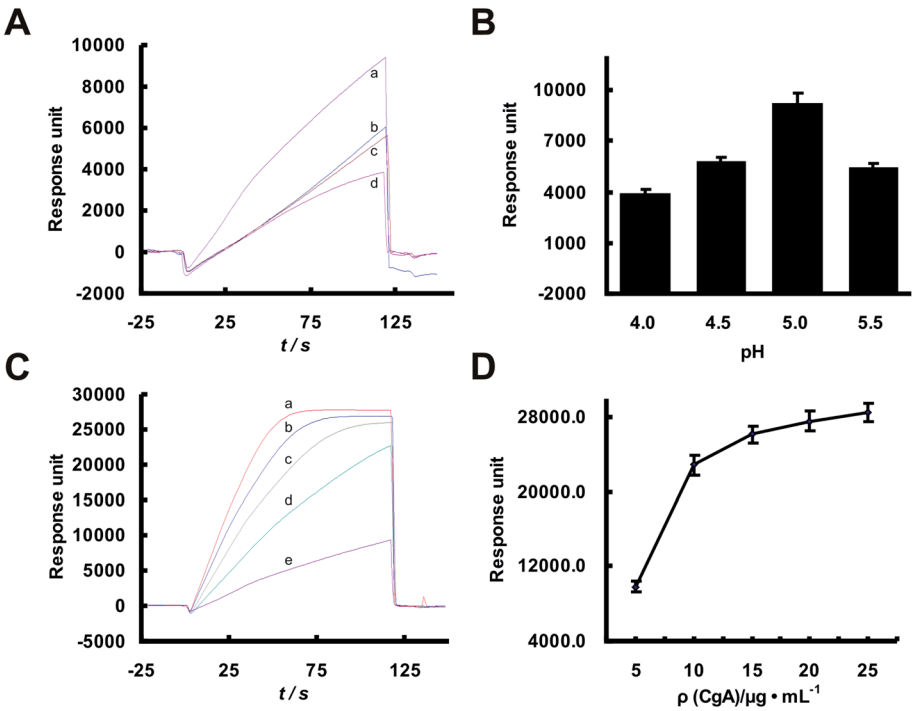

Fig. 1 Optimal pH and concentration for CgA-Ab interaction with CM5 sensor chips. (A and B) The CgA-Ab was prepared with different pH of sodium acetate (10 mM, (a) 5.0, (b) 4.5, (c) 5.5, (d) 4.0), and CgA-Ab (5 μg mL^{-1}) were then injected into the FC2 of the CM5 sensor chip with the same concentration (5 μg mL^{-1}). The sensorgrams (A) and quantified data (B) were shown; (C and D) various concentrations of CgA-Ab ((a) 25, (b) 20, (c) 15, (d) 10, (e) 5 μg mL^{-1}) diluted in sodium acetate with optimal pH (5.0) were injected into FC2. The sensorgrams (C) and quantified data (D) were shown.

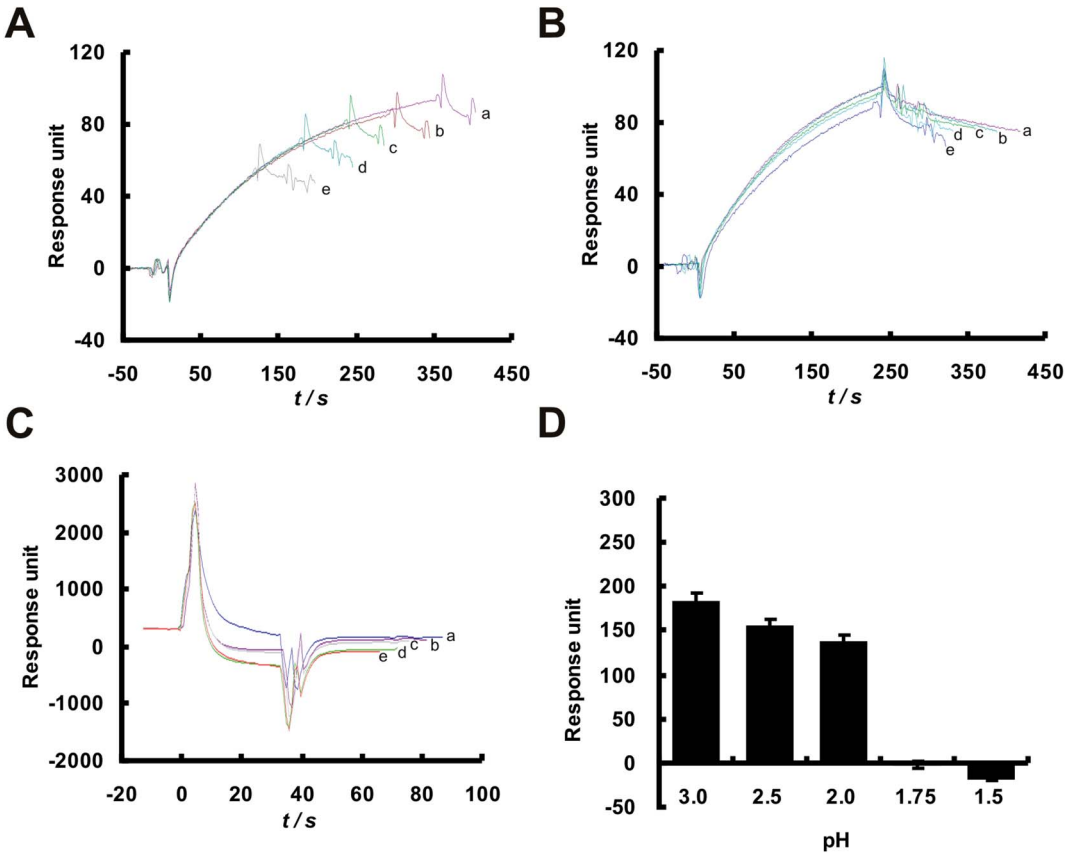

Fig. 3 Optimal binding conditions for the CgA interaction with CgA-Ab-CM5 sensor chip. (A) As shown in the sensorgrams, CgA (5.9 ng mL^{-1}) was injected into CgA-Ab-CM5 at a flow rate of 10 μL min^{-1} and quit at a different time ((a) 360 s, (b) 300 s, (c) 240 s, (d) 180 s, (e) 120 s); (B) as shown in the sensorgrams, CgA (5.9 ng mL^{-1}) was injected into CgA-Ab-CM5 at a different flow rate ((a) 5, (b) 10, (c) 20, (d) 30, (e) 40 μL min^{-1}) and quit at a 240 s. (C and D): as shown in the sensorgrams, different pH ((a) 3.0, (b) 2.5, (c) 2.0, (d) 1.75, (e) 1.5) of regeneration buffer was injected into CgA-Ab-CM5 at a flow rate of 30 μL min^{-1} for 30 seconds after its interaction with CgA (5.9 ng mL^{-1}).

concentration of CgA-Ab at 10 ng mL^{-1} due to adequate RU without wasting ligands.

3.2 Immobilization of CgA-Ab on the CM5 sensor chip

In the activation process, the surface matrix of flow channels was activated by injection of a mixture of 0.4 M EDC and 0.1 M NHS (1 : 1, v/v, Fig. 2a). Then, the coating antibody (10 μg mL^{-1}) was injected within the optimal sodium acetate (pH = 5.0) as determined above in the immobilization process (Fig. 2b). After coupling, the deactivation process was performed by injecting ethanolamine–HCl to wash out and block the excess carboxyl dextran (Fig. 2c). The immobilization signal was calculated by subtracting the RU value of the baseline from RU after immobilization. As shown in Fig. 2, the final immobilization signal of CgA-Ab-CM5 reached 2140 RU after the activation–immobilization–deactivation cycle.

3.3 Optimization of the binding and regenerating conditions

Generally, there are three steps during the detection and analysis of the sample. The first step is the association, where the analyte CgA quickly binds with the coating CgA-Ab-CM5, and RU increases sharply. The second step is a transient plateau, in which all binding sites are occupied with analytes. In the last step, analytes dissociate from ligands, and RU decreases gradually.[17] RU will not increase if a reaction plateau has occurred after sufficient analyte injection. Thus, with a limited sample, flow rate and binding time are the two interactional factors that should be optimized. For the binding time test, the prepared CgA sample (5.9 ng mL^{-1}) was injected at a flow rate of 10 μL min^{-1} and quit at a different time (360, 300, 240, 180, 120 s). As shown in Fig. 3A, RU increases along with the binding time. However, when the binding time is over 240 s, the slope of tangent on the curve is lower than 1, suggesting that the increase in RU caused by the addition of the sample is limited in this condition. So, 240 s was determined as the optimal binding time as analytes can react with ligands adequately without wasting the sample. We next fixed the binding time at 240 s and injected the CgA sample (5.9 ng mL^{-1}) at a different flow rate (5, 10, 20, 30, 40 μL min^{-1}). The optimal flow rate of 30 μL min^{-1} was determined based on RU. It is in accordance with the typical injecting flow rate of analytes in other trials of SPR.[16,18]

After each detection, the CgA binding to the CgA-Ab-CM5 sensor chip should be washed out by a regeneration buffer. Since the improper pH of the regeneration buffer has been

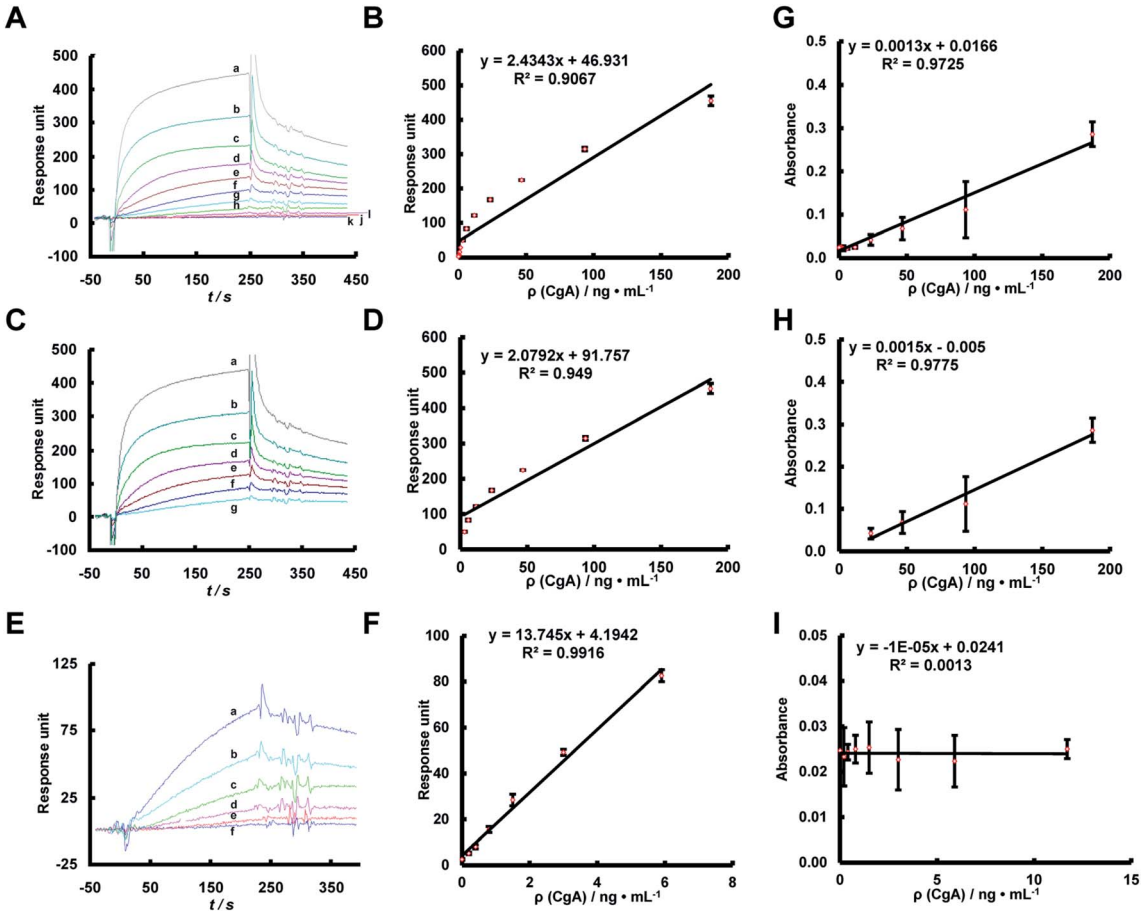

Fig. 4 Quantification of CgA with CgA-Ab-CM5 and ELISA. (A and B) sensorgrams (A) and calibration curves (B) of different concentration of CgA (0.2–187 ng mL^{-1}) analyzed by CgA-Ab-CM5; *c*/(ng mL^{-1}): (a) 187.0, (b) 93.5, (c) 46.7, (d). 23.4, (e). 11.7, (f) 5.9, (g) 3.0, (h) 1.5, (i) 0.8, (j) 0.4, (k) 0.2. (C and D) sensorgrams (C) and calibration curves (D) of different concentration of CgA (3.0–187 ng mL^{-1}) analyzed by CgA-Ab-CM5; *c*/(ng mL^{-1}): (a) 187.0, (b) 93.5, (c) 46.7, (d) 23.4, (e) 11.7, (f) 5.9, (g) 3.0. (E and F) Sensorgrams (E) and calibration curves (F) of different concentration of CgA (0.2–5.9 ng mL^{-1}) analyzed by CgA-Ab-CM5; *c*/(ng mL^{-1}): (a) 5.9, (b) 3.0, (c) 1.5, (d) 0.8, (e) 0.4, (f) 0.2. (G–I) Calibration curves of different concentration of CgA ((G): 0.2–187 ng mL^{-1}; (H): 23.4–187 ng mL^{-1}; (I): 0.2–11.7 ng mL^{-1}) analyzed by ELISA.

found to affect the baseline RU[19] and even damage the reproducibility of the sensor chip,[20] it is necessary to optimize the regenerating pH to ensure authentic results for each measurement. We injected glycine–HCl of different pH values (3.0, 2.5, 2.0, 1.75, 1.5) into the flow channel at a flow rate of 30 μL min^{-1} for 30 seconds to regenerate the sensor chip after each measurement. The optimal pH of 1.75 was chosen according to Fig. 3C and D due to minimizing the post-measurement RU. In

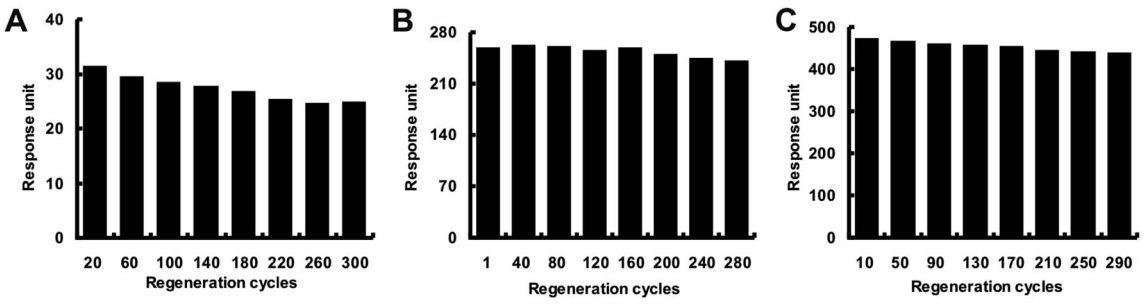

Fig. 5 Reproducibility and reusable times of CgA-Ab-CM5 chip with different concentrations of CgA. CgA at different concentrations (5.9, 42, 187 ng mL^{-1}) were injected into CgA-Ab-CM5 chip at a flow rate of 30 μL min^{-1} for 4 minutes. Then the surfaces were regenerated each time with the regeneration solution (1 M glycine–HCl, pH 1.75) at a flow rate of 30 μL min^{-1} for 30 seconds. The RU value of the CgA-Ab-CM5 chip with CgA at 5.9 ng mL^{-1} (A), 42 ng mL^{-1} (B), and 187 ng mL^{-1} (C) was tested after the indicated cycles of regeneration.

summary, we chose the binding time of 240 s, and flow rate of 30 μL min^{-1} as the optimal binding conditions, and a pH of 1.75 as the optimal regeneration conditions.

3.4 Quantification of CgA with CgA-Ab-CM5 and ELISA

Under the optimal experimental conditions determined above, CgA at different concentrations was detected by the CgA-Ab-CM5 sensor chip. As shown in Fig. 4A and B, sensorgrams and calibration curves indicated that RU was enhanced with increasing the concentration of analyte with a quantification range of 0.2–187 ng mL^{-1} (R^2 = 0.9067, Fig. 4A and B). Furthermore, we investigated signal strength variation with CgA concentration from 3.0 to 187 ng mL^{-1} (R^2 = 0.949, Fig. 4C and D) and from 0.2 to 5.9 ng mL^{-1} (R^2 = 0.9916, Fig. 4E and F). Meanwhile, we also use the ELISA to determine the CgA. The ELISA showed a detection range of 23.4–187 ng mL^{-1} (R^2 = 0.9775, Fig. 4G and H). However, ELISA could not differentiate the range of 0.2–11.7 ng mL^{-1} (R^2 = 0.0013, Fig. 4G and I). It suggested that SPR is a sensitive method that can measure a lower level of CgA accurately when compared with ELISA.

Due to various test methods and post-translational modifications of CgA, studies have reported a wide range of normal CgA levels from 14 to 233 ng mL^{-1} by RIA and ELISA.[21,22] In pathological conditions, elevated CgA concentrations in many kinds of tumors are involved in our detection range of SPR, *e.g.*, pheochromocytoma with 116 ng mL^{-1},[4] large cell lung carcinoma with 180 ng mL^{-1},[23] pancreatic ductal adenocarcinoma with 138 ng mL^{-1},[5] *etc.* Although CgA in some NETs like carcinoid tumors could reach more than 700 ng mL^{-1},[24] which might exceed the upper limit of detection, it can be solved by the dilution of the sample. NETs are rare diseases with a low incidence rate of 6.98 per 100 000, and the levels of CgA in blood is one of the standard golden tests for NETs.[3,4] Thus, further studies are needed to test the blood levels of CgA from NET patients by using the established SPR-based BIAcore techniques. In summary, the CgA-Ab-CM5 sensor chip detected the CgA with a quantification range of 0.2–187 ng mL^{-1}.

3.5 Reproducibility and reusable times of CgA-Ab-CM5 sensor chip

To evaluate whether the quantification of CgA by SPR is stable and repeatable, regeneration studies were conducted with three different concentrations of CgA (Fig. 5). The CgA-Ab-CM5 chip was regenerated using glycine-HCl for a total of 300 times. Over the regeneration cycles, the RU values were almost the same under a specified concentration of CgA, suggesting the high reproducibility of the approach. Conventional methods of quantifying CgA are costly, time-consuming, and require high skills. Hence, it would translate into a better cost-effectiveness ratio over classic ELISA or RIA. In addition, the advantages of SPR were also shown in the measurement of other biomarkers. For example, the determination of 3-Nitrotyrosine by SPR was developed to compare with ELISA and was demonstrated to be more advantageous in the detection limit.[25] The detection of α-cyclopiazonic acid and insulin autoantibodies by SPR were validated to be in high accordance with ELISA or RIA, respectively, but with advantages of label-free and time-saving.[26,27] In summary, the CgA-Ab-CM5 sensor chip showed high reproducibility and good reusable times to detect CgA.

4 Conclusions

The SPR-based CgA-Ab-CM5 sensor chip displayed its simplicity of operator, high sensitivity, and reliability in detecting CgA with a detection range of 0.2–187 ng mL^{-1}, which covers the range of most diseases. Moreover, the CgA-Ab-CM5 sensor chip can get the results in real-time and be reused more than 300 times with one sensor chip, which meets the requirements for monitoring the CgA level in clinical samples. Further studies are needed to validate blood CgA levels using the CgA-Ab-CM5 sensor chip to diagnose and predict the prognosis of diseases.

Abbreviations

CgA	Chromogranin A
CgA-Ab	CgA antibody
ELISA	Enzyme-linked immunosorbent assay
EDC	*N*-Ethyl-*N*′-(3-diethylaminopropyl) carbodiimide
FC1	Flow channel 1
FC2	Flow channel 2
IRMA	Immunoradiometric assay
NETs	Neuroendocrine tumors
NHS	*N*-Hydroxysuccinimide
RU	Response unit
RIA	Radioimmunoassay
SPR	Surface plasmon resonance

Funding

This study is supported by the Natural Science Fund of China (81873584, U1702281, 81670551) and the Science and Technology Support Program of Sichuan province (2021YFS0147).

Author contributions

JG and CT conceived and supervised the study; YX, YT, XQ, CZ, RL and ZH performed experiments; YX, XQ, and HT analyzed the data; YX, YT, XQ, and JG wrote the manuscript with input from all the authors.

Conflicts of interest

All authors declare no conflict of interest.

References

1 L. Taupenot, K. L. Harper and D. T. O'Connor, *N. Engl. J. Med.*, 2003, **348**, 1134–1149.
2 P. Banks and K. Helle, *Biochem. J.*, 1965, **97**, 40C–41C.
3 D. T. O'Connor and K. N. Bernstein, *N. Engl. J. Med.*, 1984, **311**, 764–770.

4 R. Bilek, P. Vlcek, L. Safarik, D. Michalsky, K. Novak, J. Duskova, E. Vaclavikova, J. Widimsky Jr and T. Zelinka, *Cancers*, 2019, **11**, 386.
5 S. H. Lee, J. H. Jo, Y. J. Kim, H. S. Lee, M. J. Chung, J. Y. Park, S. Bang, S. W. Park and S. Y. Song, *Pancreas*, 2019, **48**, 662–669.
6 P. Verderio, R. Dittadi, E. Marubini, S. Pizzamiglio, M. Gion, L. De Apollonia, A. Paradiso and G. Italian, Network for Quality Assessment of Tumor Biomarkers, *Clin. Chem. Lab. Med.*, 2007, **45**, 1244–1250.
7 R. Ramachandran, P. Bech, K. G. Murphy, M. E. Caplin, M. Patel, S. Vohra, M. S. Khan, W. S. Dhillo, R. Sharma, F. F. Palazzo, Z. Win, T. Tan, B. Khoo, K. Meeran, A. Frilling, M. A. Ghatei, S. R. Bloom and N. M. Martin, *J. Clin. Endocrinol. Metab.*, 2015, **100**, 1520–1528.
8 C. Nogues, H. Leh, C. G. Langendorf, R. H. Law, A. M. Buckle and M. Buckle, *PLoS One*, 2010, **5**, e12152.
9 J. S. Mitchell, T. E. Lowe and J. R. Ingram, *Analyst*, 2009, **134**, 380–386.
10 M. C. Zatelli, M. Torta, A. Leon, M. R. Ambrosio, M. Gion, P. Tomassetti, F. De Braud, G. Delle Fave, L. Dogliotti, E. C. degli Uberti and G. Italian CromaNet Working, *Endocr.-Relat. Cancer*, 2007, **14**, 473–482.
11 Y. Zhao, R. J. Tong, F. Xia and Y. Peng, *Biosens. Bioelectron.*, 2019, **142**, 111505.
12 D. G. Drescher, D. Selvakumar and M. J. Drescher, *Adv. Protein Chem. Struct. Biol.*, 2018, **110**, 1–30.
13 A. Jebelli, F. Oroojalian, F. Fathi, A. Mokhtarzadeh and M. Guardia, *Biosens. Bioelectron.*, 2020, **169**, 112599.
14 J. Gao, H. Tong, Z. Huang, R. Liu, X. Li, O. Qiang and C. Tang, *Anal. Methods*, 2013, **5**, 3201–3206.
15 J. Gao, R. Liu and H. Tong, *Chem. Res. Chin. Univ.*, 2010, **31**, 1327–1331.
16 Y. Fa, M. Guan, H. Zhao, F. Li and H. Liu, *Anal. Methods*, 2019, **11**, 3061–3065.
17 S. Fan, C. Li, J. Ma, Z. Meng, L. Zhao and Y. Zhang, *Anal. Methods*, 2021, **13**, 1278–1285.
18 L. Bar, C. Nguyen, M. Galibert, F. Santos-Schneider, G. Aldrian, J. Dejeu, R. Lartia, L. Coche-Guerente, F. Molina and D. Boturyn, *Anal. Chem.*, 2021, **93**, 6865–6872.
19 A. W. Drake and S. L. Klakamp, *J. Immunol. Methods*, 2011, **371**, 165–169.
20 J. H. Qu, K. Leirs, R. Escudero, Z. Strmsek, R. Jerala, D. Spasic and J. Lammertyn, *Nanomaterials*, 2021, **11**, 186.
21 E. Blind, H. Schmidt-Gayk, H. P. Sinn, D. T. O'Connor and F. Raue, *Thyroid*, 1992, **2**, 5–10.
22 C. H. Hsu, L. F. Reyes, C. J. Orihuela, R. Buitrago, A. Anzueto, N. J. Soni, S. Levine, J. Peters, C. A. Hinojosa, S. Aliberti, O. Sibila, A. Rodriguez, J. D. Chalmers, I. Martin-Loeches, J. Bordon, J. Blanquer, F. Sanz, P. J. Marcos, J. Rello, J. Sole-Violan and M. I. Restrepo, *Biomarkers*, 2015, **20**, 171–176.
23 R. E. Sobol, D. T. O'Connor, J. Addison, K. Suchocki, I. Royston and L. J. Deftos, *Ann. Intern. Med.*, 1986, **105**, 698–700.
24 D. T. O'Connor and L. J. Deftos, *N. Engl. J. Med.*, 1986, **314**, 1145–1151.
25 Q. He, Y. Chen, D. Shen, X. Cui, C. Zhang, H. Yang, W. Zhong, S. A. Eremin, Y. Fang and S. Zhao, *Talanta*, 2019, **195**, 655–661.
26 Z. Hossain, M. Busman and C. M. Maragos, *Anal. Bioanal. Chem.*, 2019, **411**, 3543–3552.
27 J. Carlsson, C. Gullstrand, G. T. Westermark, J. Ludvigsson, K. Enander and B. Liedberg, *Biosens. Bioelectron.*, 2008, **24**, 882–887.